ISSN 2072-5981
doi: 10.26907/mrsej

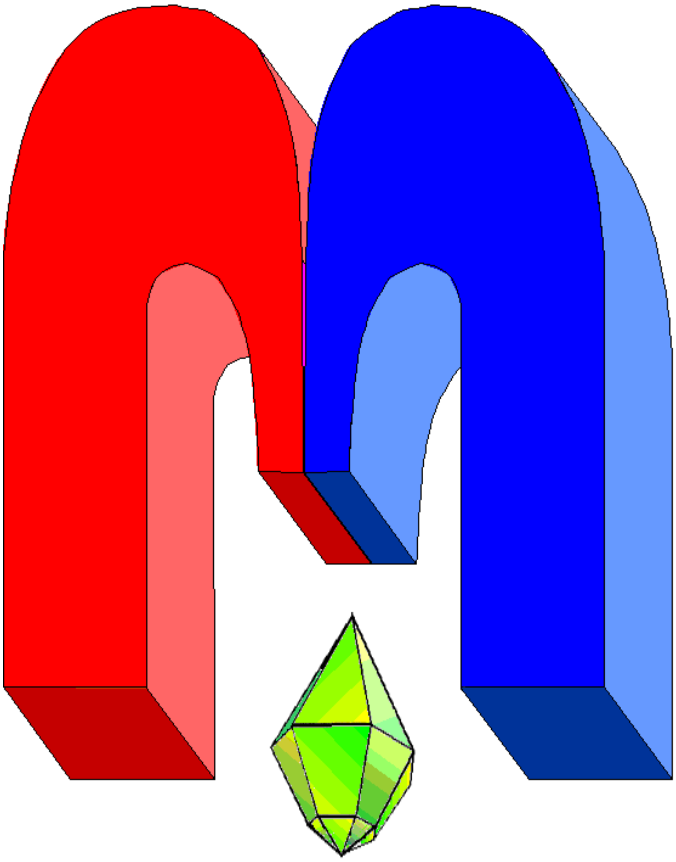

Magnetic Resonance in Solids

Electronic Journal

Volume ***26***
Issue ***2***
Article No ***24202***
1-8 pages
June, ***6***
2024
doi: **10.26907/mrsej-24202**

http://mrsej.kpfu.ru
https://mrsej.elpub.ru

Established and published by Kazan University[*]
Endorsed by International Society of Magnetic Resonance (ISMAR)
Registered by Russian Federation Committee on Press (#015140),
August 2, 1996
First Issue appeared on July 25, 1997

"*Magnetic Resonance in Solids. Electronic Journal*" (**MRSej**) is a peer-reviewed, all electronic journal, publishing articles which meet the highest standards of scientific quality in the field of basic research of a magnetic resonance in solids and related phenomena.

Indexed and abstracted by
Web of Science (*ESCI*, Clarivate Analytics, from 2015),
Scopus (Elsevier, from 2012), *RusIndexSC* (*eLibrary*, from 2006), *Google Scholar*,
DOAJ, *ROAD*, *CyberLeninka* (from 2006), *SCImago Journal & Country Rank*, etc.

Invited Editor of Special Issue[‡]: Eduard Baibekov (KFU, Kazan)

---

[*] Address: "Magnetic Resonance in Solids. Electronic Journal", Kazan Federal University; Kremlevskaya str., 18; Kazan 420008, Russia

[†] In Kazan University the Electron Paramagnetic Resonance (EPR) was discovered by Zavoisky E.K. in 1944.

[‡] Dedicated to Professor Boris Z. Malkin on the occasion of his 85th birthday

Magnetization of $LiErF_4$ dipolar magnet in monocrystalline and polycrystalline form at low temperatures[†]

G.Iu. Andreev[1,*], I.V. Romanova[1], S.L. Korableva[1], M.A. Cherosov[1], A.G. Kiiamov[1], H. Suzuki[2], M.S. Tagirov[3]

[1]Kazan Federal University, Kazan 420008, Russia

[2]Kanazawa University, Kanazawa 920-11, Japan

[3]Institute of Applied Research, Tatarstan Academy of Science, Kazan 420111, Russia

**E-mail: ujif28@mail.ru*

(Received March 30, 2024; accepted May 30, 2024; published June 6, 2019)

This work presents the results of experimental and theoretical studies of the magnetic properties of the $LiErF_4$ single crystal and powder samples at low temperatures and applied field range of 0-9 T. The magnetization was calculated in the framework of the exchange-charge model taking into account dipole-dipole and electron-deformation interactions, with the calculation of the electron-deformation parameters. The theoretical analysis presents quantitative agreement in the temperature range of 2-300 K with the magnetization measurements of the $LiErF_4$ samples.

PACS: 31.15.Ne, 75.50.-y
Keywords: magnetization, magnetoelastic interaction

1. Introduction

Concentrated rare-earth–lithium double fluorides (also tetrafluorides, $LiREF_4$, RE = Gd-Yb) have gained attention as model objects in physics of dipolar magnetism, quantum phase transitions and crystal field effects on rare-earth 3+ ions (e. g. [1–9]). Besides, their unique magnetic and optical properties are important for practical applications as optical, magnetic and magneto-optical materials, e. g., in low-temperature adiabatic demagnetization refrigeration [10–14], in high-power Faraday devices [15,16], in photonics and quantum electronics [17–19].

All $LiREF_4$ materials share the same, scheelite $CaWO_4$ type, $I4_1/a$ symmetry with RE^{3+} ions in two magnetoequivalent positions in the unit cell [1,20–22]. Rare-earth ions form a structure similar to a diamond crystal lattice [23], which makes rare-earth–lithium double fluorides a model object of order by disorder phenomena study [5,24]. The significant influence of magnetic fields on the structure of the crystal lattice of double fluorides of rare earths has been observed earlier [25–28], and this effect appears only in strong magnetic fields ($B > 1\,\mathrm{T}$). The study of magnetic properties of $LiREF_4$ single crystals is an important problem for the development of the theory of magnetoelastic effects in magnetically concentrated crystals containing rare-earth ions [28].

$LiErF_4$ is an XY antiferromagnet with Neel temperature $T_\mathrm{N} = 373(5)\,\mathrm{mK}$ [29], easy plane is orthogonal to c axis. The energy spectrum of the Er^{3+} ion in the concentrated erbium tetrafluoride is shown in Table 2. The ground multiplet is $^4I_{15/2}$, its ground state is a Kramers doublet of Γ_{78} symmetry [4]. The g-factors have the values of $g_\parallel = 3.173(3)$, $g_\perp = 8.105(12)$ [30]. The linear magnetostriction of $LiErF_4$ single crystal in the field range of 0-3 T applied along the [100] axis has the order of $\Delta l/l \sim 10^{-4}$ [26]. A giant magnetocaloric effect was observed below the temperature of 2 K [31]. The neutron spectroscopy and specific heat study at low and ultra-low (sub-kelvin) temperatures was carried by Kraemer et al. [29], the magnetic phase diagram

---

[†] This paper is dedicated to Professor Boris Z. Malkin, who made a significant contribution to the field of magnetic radio spectroscopy in Kazan University, on the occasion of his 85th birthday.

was plotted and this system was found to have a huge interest for a research of a quantum phase transition. However, the magnetization of LiErF$_4$ single crystal as a function of the magnetic field, especially in strong magnetic fields (up to 5 T) and in the paramagnetic state at low temperatures (down to 2 K), has not been investigated as of now.

2. Experimental details

Single crystal LiErF$_4$ samples were grown in Kazan Federal University by the Bridgman-Stockbarger method. The resistive heater and thermal insulators were made of high-purity graphite. The crystals were grown at high vacuum (10^{-3} Pa) with a pulling rate of 1 mm/h using graphite crucibles for [100]-oriented boules. Single crystals were grown from compounds of 50 mol% ErF$_3$ (99.99 %) and 50 mol% LiF (99.99 %) at 850°C. These parameters are consistent with the growing conditions selected by Thoma et al. [21]. Powder LiErF$_4$ samples were synthesized in Kazan Federal University by sintering powders of fluorides taken in proportions according to the phase diagrams [21, 32] in the same oven as the single crystal samples. Powders of LiF (99.99 %) and ErF$_3$ (99.99 %) were mixed in an agate mortar and dried in the vacuum of $4 \cdot 10^{-3}$ Pa for 2 h at 150°C in a vitreous carbon crucible to prevent the hydrolysis. The synthesis was continued in the same crucible at 600°C in an atmosphere of high purity Ar (99.98 %) for 18 h. X-ray diffraction measurements were performed on a *Bruker D8 ADVANCE* diffractometer using Cu Kα radiation with a wavelength $\lambda = 1.5418$ Å to assess the crystallinity of the samples and for orientation of the single crystal samples. The comparison of the experimental powder LiErF$_4$ sample diffractogram and calculated one (Fig. 1) indicates no crystalline phases other than erbium–lithium double fluoride.

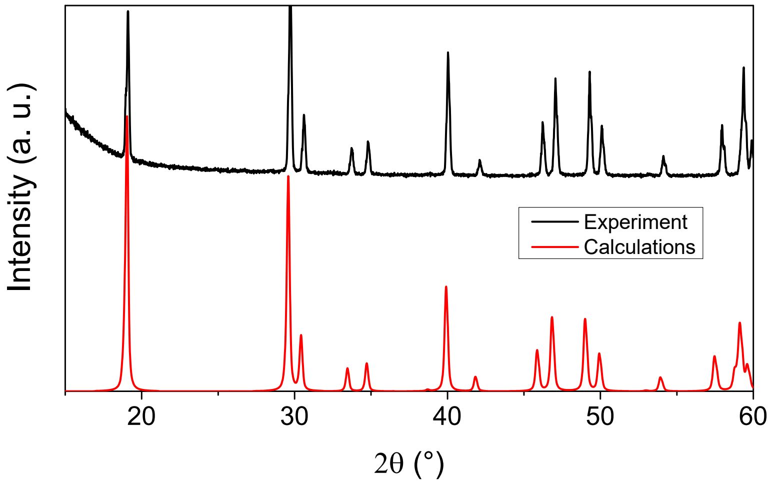

Figure 1. Experimental (top) and calculated (bottom) diffractograms of the powder LiErF$_4$ sample. Calculations were performed using *MAUD* software [33] with data taken from [20].

The magnetization of the powder samples was measured on a vibrating sample magnetometer *VSM* of *Physical Properties Measurement System (PPMS®)*, automated low-temperature and magnet system *(Quantum Design)*, which allows DC magnetic measurements in the applied field range of 0-9 T and temperature range of 2-300 K (Kazan, Russia). The temperature dependencies of the magnetization of single crystals in the temperature range of 2-300 K and the dependencies of the magnetization on the magnetic field in the interval of 0-5 T applied along and perpendicular to the *c*-axis were measured with a DC-SQUID magnetometer *MPSM-2* (*Quantum Design*;

Kanazawa, Japan). Ball-shaped $\mathrm{LiErF_4}$ samples of 2 mm diameter were used in the single-crystal magnetization measurements.

3. Theoretical analysis

In the presence of an applied magnetic field $\mathbf{B}$, we write the Hamiltonian of a single Er^{3+} ion operating in the space of the ground multiplet states in the following form:

$$\hat{\mathcal{H}} = \hat{\mathcal{H}}_{\mathrm{cf}} + \hat{\mathcal{H}}_{\mathrm{Z}} + \sum_{\alpha\beta} \hat{V}'_{\alpha\beta} e_{\alpha\beta} + \sum_{\alpha,s} \hat{V}''_{\alpha}(s) w_{\alpha}(s). \tag{1}$$

$\hat{\mathcal{H}}_{cf}$ is the crystal field Hamiltonian

$$\begin{aligned}\hat{\mathcal{H}}_{\mathrm{cf}} = {} & B_2^0 \hat{O}_2^0 + B_4^0 \hat{O}_4^0 + B_4^4 \hat{O}_4^4 + B_4^{-4} \hat{O}_4^{-4} \\ & + B_6^0 \hat{O}_6^0 + B_6^4 \hat{O}_6^4 + B_6^{-4} \hat{O}_6^{-4},\end{aligned} \tag{2}$$

determined in the crystallographic system of coordinates by the set of seven crystal field parameters B_p^k (see Table 1), $\hat{O}_p^k$ are the Stevens equivalent operators [22].

Table 1. Crystal field parameters for $\mathrm{LiErF_4}$ (in $\mathrm{cm^{-1}}$) [34].

B_2^0	B_4^0	B_6^0	B_4^4	B_4^{-4}	B_6^4	B_6^{-4}
190	−80	−2.3	−771	−667	−363	−222

$\hat{\mathcal{H}}_{\mathrm{Z}}$ is the electronic Zeeman energy

$$\hat{\mathcal{H}}_{\mathrm{Z}} = \mu_{\mathrm{B}} \sum_j \mathbf{B}_{\mathrm{loc}} \left(\hat{\mathbf{l}}_j + 2\hat{\mathbf{s}}_j \right), \tag{3}$$

where μ_{B} is the Bohr magneton, $\hat{\mathbf{l}}_j$ and $\hat{\mathbf{s}}_j$ are operators of electronic orbital and spin moments and the sum is taken over $4f$-electrons. The magnetic dipole interaction between the Er^{3+} ions is taken into account by the introduction of a local magnetic field:

$$\mathbf{B}_{\mathrm{loc}}(s) = \mathbf{B} + \sum_{s'} \left[\hat{Q}(s,s') - \frac{4\pi}{3v} N_{\mathrm{m}} \delta_{ss'} \hat{1} \right] \mathbf{M}(s'), \tag{4}$$

defined by the applied magnetic field $\mathbf{B}$, the lattice sums $\hat{Q}(s,s')$ calculated by the Ewald method ($Q_{xx}(s,s) = Q_{yy}(s,s) = 1.1702$ cm^{-3}, $Q_{xx}(s_1,s_2) = Q_{yy}(s_1,s_2) = 0.4332$ cm^{-3}, $Q_{zz}(s,s) = 0.6595$ cm^{-3}, $Q_{zz}(s_1,s_2) = 2.1335$ cm^{-3}, $s_1 \neq s_2$), the volume $v = 0.5a^2c$ of the unit cell, the demagnetization factor N_{m} and the magnetic moment $\mathbf{M}(s')$ of the ion in the s'-th sublattice. As the $\mathrm{LiErF_4}$ is a dipolar magnetic, the exchange interaction has negligible effect, thus it has not been included.

The terms $\sum_{\alpha\beta} \hat{V}'_{\alpha\beta} e_{\alpha\beta} + \sum_{\alpha,s} \hat{V}''_{\alpha}(s) w_{\alpha}(s)$ in (1) correspond to linear interactions of the rare-earth ions with the homogeneous macro- and microdeformations, respectively, where $\hat{e}$ is the deformation tensor and $w_{\alpha}(s)$ is the displacement of the s-th sublattice.

Table 2 shows the measured [4] and the calculated by diagonalizing the Hamiltonian (2) energy levels of the ground multiplet for $\mathrm{LiErF_4}$ [35].

From the equilibrium conditions, we obtain the lattice macro-deformation induced by the external magnetic field [36]:

$$\hat{e}(\mathbf{B}) = -\frac{n}{v} \hat{S} \left[\langle \hat{V} \rangle_B - \langle \hat{V} \rangle_0 \right]. \tag{5}$$

Table 2. Energy (cm^{-1}) of the Stark sublevels of the ground multiplet of the Er^{3+} ion in LiErF$_4$.

	Experiment, [4]	Calculation, this work
$\Gamma_{7,8}$	0	0
$\Gamma_{5,6}$	18	17
$\Gamma_{7,8}$	29	22
$\Gamma_{5,6}$	57	57
$\Gamma_{5,6}$	256	245
$\Gamma_{5,6}$	294	289
$\Gamma_{7,8}$	321	316
$\Gamma_{7,8}$	346	343

Here $\hat{S}$ is the compliance tensor of the lattice, $n = 2$ is the number of rare earth ions in the unit cell, and angular brackets $\langle \ldots \rangle_B$, $\langle \ldots \rangle_0$ indicate the quantum statistical averaging for $B \neq 0$ and $B = 0$, respectively, for the ion with the Hamiltonian $\hat{\mathcal{H}}_{\mathrm{cf}} + \hat{\mathcal{H}}_{\mathrm{Z}}$. Operator $\hat{V}$ presents the renormalization of the operator $\hat{V}'$ due to linear coupling of macro- and micro-deformations:

$$\hat{V} = \hat{V}' - \hat{b}\hat{a}^{-1}\hat{V}''. \tag{6}$$

Here $\hat{a}$ is the dynamic matrix of the lattice at the Brillouin zone centre, the tensors $\hat{b}_{\alpha\beta\gamma}(s)$ determine linear coupling between macro- and microdeformations.

Calculations are significantly simplified if the symmetry properties of the system are taken into account. Let us introduce linear combinations of components of the deformation tensor $e(A_g^1) = e_{zz}$, $e(A_g^2) = (e_{xx} + e_{yy})/2$, $e(B_g^1) = e_{xx} - e_{yy}$, $e(B_g^2) = e_{xy}$, $e_1(E_g) = e_{xz}$, $e_2(E_g) = e_{yz}$, which transform according to the irreducible representations $\Gamma = A_g, B_g, E_g$ of the factor group of the lattice. The magnetic field directed along the [001] axis induces only totally symmetric deformations A_g, whereas the field directed in the (001) plane induces totally symmetric and rhombic deformations B_g. In the basis of the symmetrized deformations, the operators in the electron–deformation interaction have the following form:

$$\begin{aligned} \hat{V}(A_g^\lambda) = {} & a^0_{\lambda,2}\hat{O}^0_2 + a^0_{\lambda,4}\hat{O}^0_4 + a^4_{\lambda,4}\hat{O}^4_4 + a^{-4}_{\lambda,4}\hat{\Omega}^4_4 \\ & + a^0_{\lambda,6}\hat{O}^0_6 + a^4_{\lambda,6}\hat{O}^4_6 + a^{-4}_{\lambda,6}\hat{\Omega}^4_6, \end{aligned} \tag{7}$$

$$\begin{aligned} \hat{V}(B_g^\lambda) = {} & b^2_{\lambda,2}\hat{O}^2_2 + b^{-2}_{\lambda,2}\hat{\Omega}^2_2 + b^2_{\lambda,4}\hat{O}^2_4 + b^{-2}_{\lambda,4}\hat{\Omega}^2_4 \\ & + b^2_{\lambda,6}\hat{O}^2_6 + b^{-2}_{\lambda,6}\hat{\Omega}^2_6 + b^6_{\lambda,6}\hat{O}^6_6 + b^{-6}_{\lambda,6}\hat{\Omega}^6_6. \end{aligned} \tag{8}$$

The set of $a^k_{\lambda,p}$ and $b^k_{\lambda,p}$ parameters was calculated within the framework of the exchange-charge model [37] based on the crystal field [34] and EPR spectra [38] (Table 3).

4. Results and dscussion

The magnetization M (magnetic moment per unit cell) of the powder of particles distributed equiprobably with respect to the direction of the applied field $\mathbf{B}$ can be calculated as follows:

$$M = \frac{2\mu_{\mathrm{B}} g_{\mathrm{L}}}{4\pi} \int_0^{2\pi} \mathrm{d}\phi \int_0^{\pi} \mathrm{d}\theta \sin\theta \, \frac{\mathrm{Tr}\left[\hat{\mathbf{J}} \frac{\mathbf{B}}{|\mathbf{B}|} \exp\left(-\hat{\mathcal{H}}\beta\right)\right]}{\mathrm{Tr}\left[\exp\left(-\hat{\mathcal{H}}\beta\right)\right]}. \tag{9}$$

Here, g_{L} is the Landé factor, Tr[...] is the trace of the matrix, $\beta = (k_{\mathrm{B}}T)^{-1}$ is the inverse temperature.

Table 3. Parameters of the interaction of Er^{3+} ions with deformations of A_g and B_g symmetry used in the work (in cm^{-1}).

p	k	$a^k_{1,p}$	$a^k_{2,p}$	p	k	$b^k_{1,p}$	$b^k_{2,p}$
2	0	16	−885	2	2	2045	4114
4	0	305	357	2	−2	2305	−886
4	4	2129	3228	4	2	−854	−1554
4	−4	1710	3592	4	−2	1449	1423
6	0	107	−88	6	2	−135	−528
6	4	1158	1452	6	−2	−427	−523
6	−4	502	1368	6	6	−605	−927
				6	−6	−691	−1046

In a self-consistent field approximation, the following procedure has been used to calculate the magnetization. First, the matrix of the Hamiltonian (1) with $M = 0$, $\hat{e} = \hat{0}$ and $w_\alpha(s) = 0$ is diagonalized to calculate the values of the macro- and micro-deformations $\hat{e}(\mathbf{B})$, $w_\alpha(s)$ and the magnetization M. At the next step, the obtained values of M, $\hat{e}(\mathbf{B})$ and $w_\alpha(s)$ are substituted into the Hamiltonian and the calculations are repeated.

Field dependencies of the magnetization of the powder $\mathrm{LiErF_4}$ sample calculated using formula (9) together with the experimental data at different temperatures are shown on the Fig. 2. The calculations used the value of demagnetization factor equal to $N_\mathrm{m} = 1$.

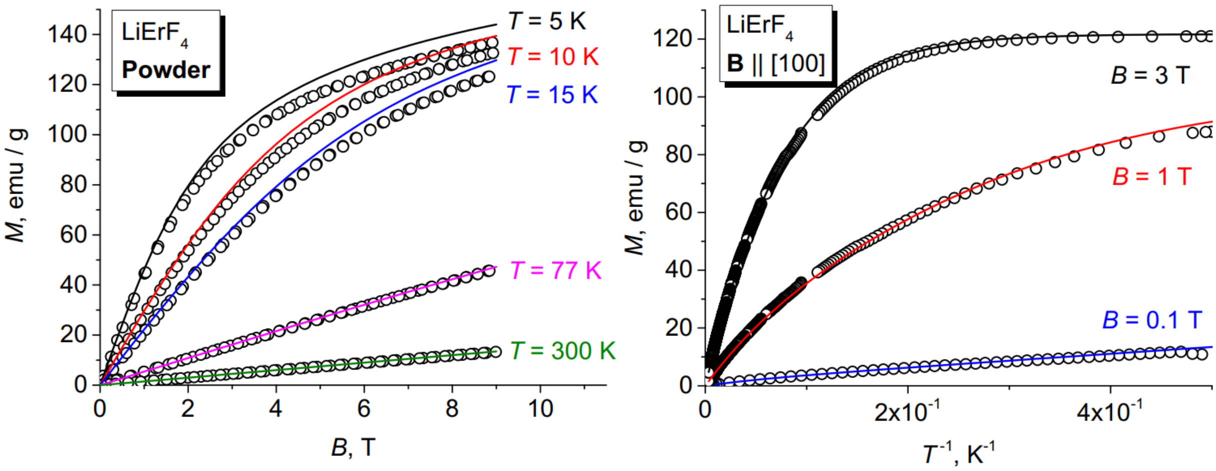

Figure 2. *Left*: Field dependencies of the magnetization of the powder $\mathrm{LiErF_4}$ sample in an external magnetic field B at different temperatures. *Right*: Inverse temperature dependencies of the magnetization of the single crystal $\mathrm{LiErF_4}$ sample in an external magnetic field $\mathbf{B} \parallel [100]$. Measurements by symbols and calculations by lines for both.

For a single crystal, the integration over all directions is unnecessary and therefore is omitted:

$$M = 2\mu_\mathrm{B} g_\mathrm{L} \frac{\mathrm{Tr}\left[\hat{\mathbf{J}}\frac{\mathbf{B}}{|\mathbf{B}|}\exp\left(-\hat{\mathcal{H}}\beta\right)\right]}{\mathrm{Tr}\left[\exp\left(-\hat{\mathcal{H}}\beta\right)\right]}. \tag{10}$$

Temperature dependencies of the magnetization of the single crystal $\mathrm{LiErF_4}$ sample were measured in the external magnetic field $\mathbf{B}$ applied along the [100] direction (Fig. 2). Field-dependencies of the magnetization of the single crystal $\mathrm{LiErF_4}$ sample were measured and calculated in the external magnetic field $\mathbf{B}$ applied along the [100] and the [001] directions (Fig. 3).

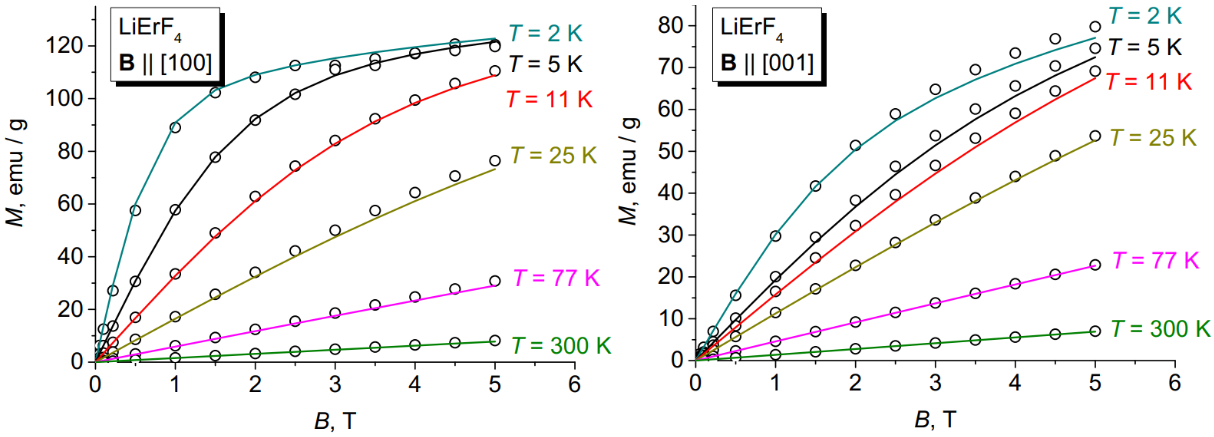

Figure 3. Field dependencies of the magnetization of the single crystal LiErF$_4$ sample in an external magnetic field **B** ∥ [100] (left) and **B** ∥ [001] (right), measured at different temperatures (symbols) and calculated ones (lines).

5. Conclusion

Magnetic properties of single crystal samples and polycrystal powder samples of LiErF$_4$ were measured and calculated taking into account the electron-deformation interaction. It has been shown that not only experimental data from this research, but also experimental Er^{3+} ion energy spectrum in the crystal field of LiErF$_4$ can be reproduced at low temperatures not only qualitatively, but also quantitatively, with a satisfactory accuracy in terms of a self-consistent theory that uses a unified set of parameters of the crystal field and electron-deformation interactions.

Acknowledgments

This work was supported by the Kazan Federal University Strategic Academic Leadership Program (PRIORITY-2030). Data processing was partially supported by RSF grant 22-12-00259.

Authors are grateful to Prof. Boris Malkin for fruitful discussions.

References

1. Aminov L. K., Malkin B. Z., Teplov M. A., in *Handbook on the Physics and Chemistry of Rare Earths*, Vol. 22, edited by Gschneider Jr. K. A., Eyring L. (Elsevier, 1996) pp. 295–506.
2. Rønnow H. M., Parthasarathy R., Jensen J., Aeppli G., Rosenbaum T. F., McMorrow D. F., *Science* **308**, 389 (2005).
3. Wendl A., Eisenlohr H., Rucker F., Duvinage C., Kleinhans M., Vojta M., Pfleiderer C., *Nature* **609**, 65 (2022).
4. Babkevich P., Finco A., Jeong M., Dalla Piazza B., Kovacevic I., Klughertz G., Krämer K. W., Kraemer C., Adroja D. T., Goremychkin E., Unruh T., Strässle T., Di Lieto A., Jensen J., Rønnow H. M., *Phys. Rev. B* **92**, 144422 (2015).
5. Babkevich P., Jeong M., Matsumoto Y., Kovacevic I., Finco A., Toft-Petersen R., Ritter C., Månsson M., Nakatsuji S., Rønnow H. M., *Phys. Rev. Lett.* **116**, 197202 (2016).
6. Kovacevic I., Babkevich P., Jeong M., Piatek J. O., Boero G., Rønnow H. M., *Phys. Rev. B* **94**, 214433 (2016).
7. McKenzie R. D., Stamp P. C. E., *Phys. Rev. B* **97**, 214430 (2018).

8. Twengström M., Bovo L., Petrenko O. A., Bramwell S. T., Henelius P., *Phys. Rev. B* **102**, 144426 (2020).
9. Dollberg T., Andresen J. C., Schechter M., *Phys. Rev. B* **105**, L180413 (2022).
10. Shirron P., Canavan E., DiPirro M., Francis J., Jackson M., Tuttle J., King T., Grabowski M., *Cryog.* **44**, 581 (2004).
11. Numazawa T., Kamiya K., Li J., Nakagome H., Shirron P., *J. Cryo. Super. Soc. Jpn* **50**, 96 (2015).
12. Xie H., Tian L., Chen Q., Sun H., Gao X., Li Z., Mo Z., Shen J., *Dalton Trans.* **50**, 17697 (2021).
13. Liu P., Yuan D., Dong C., Lin G., Víllora E. G., Zhao K., Shimamura K., Ma J., Wang J., Zhang Z., Li B., *NPG Asia Mater.* **15**, 41 (2023).
14. Andreev G. I., Romanova I. V., Morozov O. A., Korableva S. L., Batulin R. G., Glazkov V. N., Sosin S. S., *J. Magn. Magn. Mater.* **589**, 171600 (2024).
15. Vojna D., Slezák O., Lucianetti A., Mocek T., *Appl. Sci.* **9**, 3160 (2019).
16. Zhang Z., Wu Z., Zhang Z., Su L., Wu A., Li Y., Lan J., *Magnetochem.* **9**, 41 (2023).
17. Semashko V. V., Korableva S. L., Fedorov P. P., *Inorg. Mater.* **58**, 447 (2022).
18. McKenzie R. D., Libersky M., Silevitch D. M., Rosenbaum T. F., *Phys. Rev. A* **106**, 043716 (2022).
19. Berrington M. C., Sellars M. J., Longdell J. J., Rønnow H. M., Vallabhapurapu H. H., Adambukulam C., Laucht A., Ahlefeldt R. L., *Adv. Optical Mater.* **11**, 2301167 (2023).
20. Keller C., Schmutz H., *J. Inorg. Nucl. Chem.* **27**, 900 (1965).
21. Thoma R. E., Brunton G. D., Penneman R. A., Keenan T. K., *Inorg. Chem.* **9**, 1096 (1970).
22. Mollabashi L., Jalali-Asadabadi S., *Phys. Rev. B* **102**, 045120 (2020).
23. Schustereit T., Müller S. L., Schleid T., Hartenbach I., *Crystals* **1**, 244 (2011).
24. Bergman D., Alicea J., Gull E., Balents L., *Nature Phys.* **3**, 487–491 (2007).
25. Al'tshuler S. A., Krotov V. I., Malkin B. Z., *JETP Lett.* **32**, 214 (1980).
26. Bumagina L. A., Krotov V. I., Malkin B. Z., Khasanov A. K., *JETP* **53**, 792 (1981).
27. Rosenbaum T. F., Wu W., Ellman B., Yang J., Aeppli G., Reich D. H., *J. Appl. Phys.* **70**, 5946 (1991).
28. Romanova I. V., Tagirov M. S., *Magn. Reson. Solids* **21**, 19412 (2019).
29. Kraemer C., Nikseresht N., Piatek J. O., Tsyrulin N., Piazza B. D., Kiefer K., Klemke B., Rosenbaum T. F., Aeppli G., Gannarelli C., Prokes K., Podlesnyak A., Strässle T., Keller L., Zaharko O., Krämer K. W., Rønnow H. M., *Science* **336**, 1416 (2012).
30. Sattler J. P., Nemarich J., *Phys. Rev. B* **4**, 1 (1971).

31. Mo Z., Gong J., Xie H., Zhang L., Fu Q., Gao X., Li Z., Shen J., *Chin. Phys. B* **32**, 027503 (2023).

32. Fedorov P. P., Semashko V. V., Korableva S. L., *Inorg. Mater.* **58**, 233 (2022).

33. Lutterotti L., Matthies S., Wenk H.-R., Schultz A., Richardson J., *J. Appl. Phys.* **81**, 594 (1997).

34. Malkin B. Z., in *Spectroscopy of Solids Containing Rare Earth Ions*, Modern Problems in Condensed Matter Sciences, Vol. 21, edited by Kaplyanskii A. A., Macfarlane R. M. (Elsevier, 1987) Chap. 2, pp. 13–50.

35. Al'tshuler S. A., Kozyrev B. M., *Electron Paramagnetic Resonance in Compounds of Transition Elements*, 2nd ed. (John Wiley & Sons, 1974) 589 p.

36. Nuzhina D. S., Romanova I. V., *Magn. Reson. Solids* **18**, 16205 (2016).

37. Aminov L. K., Malkin B. Z., *Dinamika i Kinetika Electronnykh i Spinovykh Vozbuzhdeniy v Paramagnitnykh Kristallakh* (Kazan State University, Kazan, 2008) 182 p. [In Russian].

38. Aminov L. K., Ershova A. A., Zverev D. G., Korableva S. L., Kurkin I. N., Malkin B. Z., *Appl. Magn. Reson.* **33**, 351 (2008).